Numerical simulation of interactions between TBM-driven tunnel construction and pile foundations

J. Ninic, J. Stascheit & G. Meschke
Institute for Structural Mechanics, Ruhr-University Bochum, Germany

Abstract

This paper is concerned with the modelling of interactions between soil and existing building infrastructure within a 3D-simulation model for shield tunnelling. Resulting ground deformations and possible damage of existing building and its foundation is to be evaluated, in order to limit the risk of damage on existing structure and to design mitigation measures. Special emphasis is placed on the modelling of pile foundations and the analysis of the interactions between the piles and the construction process. Piles are represented by means of embedded beam elements that interact with the soil elements through a frictional contact algorithm. A comparative study investigates the effect of the mechanized tunnel excavation on ground settlements and pile.

1 INTRODUCTION

Traffic congestion and environmental factors are creating a demand for greater utilization of underground space in urban areas. Construction projects are being carried out ever more frequently under difficult conditions which may involve multiple constraints and potential conflicts arising from nearby infrastructure or other uses of the underground space, high risks of negative effects on third parties and unfavourable geology involving soft ground. The construction methods used in shallow soft ground when tunnelling beneath the water table must ensure that surface movements remain within acceptable limits. In mechanized tunnelling surface settlements ahead, along and behind the TBM, resulting from interactions between the face support, the conical TBM, the tail void grouting and the lining with the surrounding partially or fully saturated soil, may occur and have to be controlled by the appropriate choice of support measures.

Interactions between the tunnel construction process, the soil and existing building infrastructure in urban areas resulting in ground deformations and possible damage of existing buildings need to be evaluated. Thus, reliable prognoses of potential building and foundation damage induced by ground movements are a necessary prerequisite for the design and a valuable tool for decisions to be made during the construction of shield driven tunnels.

A form of tunnel-soil-structure interaction that has recently received much attention concerns the effect of tunnelling-induced ground movements on piles. This is mainly attributed to the fact that more tunnels are being excavated close to piled foundations (Lee et al., 1994, Coutts & Wang, 2000, Tham & Deutscher, 2000) which consequently results in additional lateral and vertical forces induced in the pile.

Current methods of analysing pile performance subjected to tunnelling induced ground movement involves a two-stage uncoupled approach where green field soil movements are approximated by a quasi-analytical method (Loganathan & Poulos, 1998), subsequently applying the obtained deformations on soil elements surrounding the pile via boundary element programs (Chen et al., 1999, Loganathan et al., 2001). This simple approach, however, does not account for coupled interaction where induced pile axial loads could result in additional bending moments (Chen & Poulos, 1999).

3D finite element (FE) studies by Mroueh & Shahrour (2002) and field data from Coutts & Wang (2000) show that the most severe loading on a close proximity pile would correspond to the tunnel face passing the pile location. Plane strain tunnel excavation is commonly simulated using the FE method by various techniques such as the Convergence Confinement Method (Panet & Guenot, 1982), Volume Loss Method and Gap Parameter Method (Lee et al., 1992) where the soil convergence around the tunnel is simulated by releasing in-situ soil stresses from equilibrium conditions, hence the term “stress based”. This shortcoming is partly improved by using advanced soil constitutive models as in Lee & Rowe (1989), Stallebrass et al. (1996), Addenbrooke et al. (1997), Simpson (1996). As noted by Stallebrass et al. (1996) and observed in NATM tunnelling studies by Dasari et al. (1996), the inclusion of advanced soil models have only resulted in limited success. Soil-pile interactions have been modelled using an embedded pile approach by Engin et al. (2008).

2 FINITE ELEMENT REPRESENTATION OF PILES

A finite element formulation has been developed to describe the interaction of piles with the surrounding soil. In soil-pile interaction problems, pile behaviour is best characterized using beam elements specially to capture nonlinear deformation and force distributions. The soil response, on the other hand, is more effectively described using solid continuum based elements. In the formulation presented in this paper the pile is considered as a 2-node beam with 6 degrees of freedom per node that can cross a 20-node hexahedral element at any place with any arbitrary orientation. The background of this strategy is to enhance soil-pile interaction modelling capabilities through the direct integration of beam-column and solid type models. The pile-soil interaction at the pile skin is described by means of a 3D frictional point-to-point contact formulation, where each pile integration point has its contact partner in the soil element. The contact detection strategy provides, for each pile element integration point, a target soil element and the coordinates of a respective local point in that element, as shown in Figure 1.This procedure allows to model pile groups independent from the discretisation of the soil considering friction between the pile skin and the surrounding soil.

The beam-solid contact formulation is based upon a geometric constraint that controls the interaction between two bodies. The contact condition interrelates the geometric distance between the two bodies, denoted as gap g, and the corresponding normal contact force between the bodies, denoted as σ_N, in the contact point is stated in terms of Kuhn-Tucker optimality conditions, characteristic of problems involving inequality constrains (Luenberger, 1984).

$$\begin{aligned} & g \geqslant 0 \\ & S_N \geqslant 0 \\ & S_N \cdot g = 0 \end{aligned} \tag{1}$$

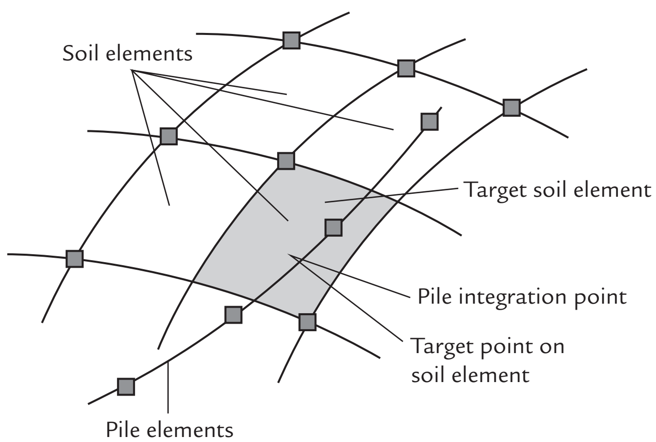

Figure 1 Representation of contact detection strategy. Pile represented by 2-node beam element crosses in arbitrary position soil element.

These conditions state that if the bodies are in contact and a positive normal contact force exists, the gap has to be zero. If the bodies are not in contact, the gap is greater than zero. This second case is exempted from this formulation, since the pile is embedded in the soil such that any relative movement between soil and pile would result in a violation of the compatibility conditions. Inadmissible states include a negative gap, which implies penetration, and a negative contact force, which forces contact release.

The frictional contact formulation is developed using the contact constraint $g=0$ and accounting for relative movements between the bodies. The total virtual work of internal, external and contact forces must be equal to zero

$$G^c(u, \delta u) = \int_{\Gamma_c} [\sigma_N \delta g + \sigma_T \delta u_T] d\Gamma \tag{2}$$

$G^c(u, \delta u)$ is a contribution to virtual work with respect to the contact constraint, $g=0$. It is given as:

$$G^c(u, \delta u) = \int_{\Gamma_c} [\sigma_N \delta g + \sigma_T \delta u_T] d\Gamma \tag{3}$$

where σ_N and σ_T are normal and tangential stresses in the contact point and δg and δu_T are normal and tangential virtual displacements, respectively. For the constrained minimization of total virtual energy the penalty method is used.

The inclusion of frictional slip in the contact formulation requires special consideration. Slip is considered as the relative movement of a slave node on the beam surface. Frictional response is introduced using the Coulomb friction law, which requires the following conditions in addition to the Kuhn-Trucker conditions summarized in (1):

$$\begin{aligned} & \Phi(\sigma_N, \sigma_T) = \|\sigma_T\| - \mu\sigma_N \leq 0 \\ & \dot{u}_T = \dot{\gamma} \frac{\sigma_T}{\|\sigma_T\|} \\ & \dot{\gamma} \geq 0 \\ & \dot{\gamma} \cdot \Phi = 0 \end{aligned} \tag{4}$$

In (4.1), Φ is the slip function and μ is the friction coefficient.

Conditions (4.2–4.4) imply that the tangential slip u_T is zero when the tangential stress is less than

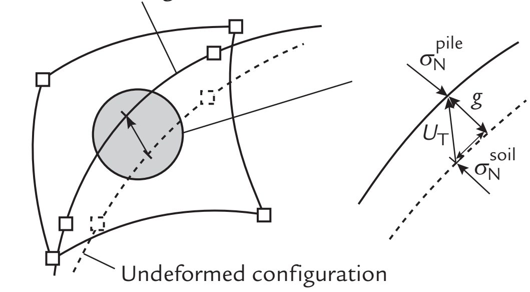

Figure 2 Definition of gap displacement

AQ

the Coulomb limit and that any tangential slip that does occur is collinear with the frictional stress. In (4.2–4.4) the co-linearity of the slip displacement u_T and the frictional stress σ_T is expressed in rate form, effectively changing the frictional law to one of an evolutionary type (Laursen, 2002).

For the numerical integration of the rate equations (4), the Newmark algorithm is used to calculate the frictional tractions at time t_{n+1}. The problem is solved through the introduction of a trial state and a subsequent return map, as is commonly employed in the integration of elasto-plastic equations. The algorithm is given below: first, the trial state is computed assuming no slip during the increment.

$$\begin{aligned} &\sigma_{\mathrm{N}n+1} = e_{\mathrm{N}} \left\langle g_{n+1} \right\rangle \\ &\sigma^{\mathrm{trial}}_{\mathrm{T}n+1} = \sigma_{\mathrm{T}n} + e_{\mathrm{N}} \Delta u_{\mathrm{T}} \\ &\sigma^{\mathrm{trial}}_{\mathrm{T}n+1} = \left\| \sigma^{\mathrm{trial}}_{\mathrm{T}n+1} \right\| - \mu \cdot \sigma_{\mathrm{N}n+1} \end{aligned} \tag{5}$$

In this equation, e_N is a penalty parameter. The slip condition (4.1) is then checked and, finally, the frictional tractions σ_T are calculated based upon equation (6):

$$\sigma_{\mathrm{T}n+1} = \begin{Bmatrix} \sigma^{\mathrm{trial}}_{\mathrm{T}n+1} & \Phi^{\mathrm{trial}}_{n+1} < 0 \\ \mu \sigma_{\mathrm{N}n+1} \dfrac{\sigma^{\mathrm{trial}}_{\mathrm{T}n+1}}{\left\| \sigma^{\mathrm{trial}}_{\mathrm{T}n+1} \right\|} & \Phi^{\mathrm{trial}}_{n+1} \geq 0 \end{Bmatrix} \tag{6}$$

The above return mapping scheme is very simple due to the elementary friction law chosen and it is readily extended to include hardening and softening effects. Importantly, the integration scheme of (5) and (6) is by construction frame invariant, because is performed within the slip advanced basis.

3 SHIELD DRIVEN TUNNELLING

The shield tunnelling process is modelled using numerical simulation model (ekate) developed in the framework of the European research project Technology Innovation in Underground Construction (TUNCONSTRUCT) for the simulation of shield driven tunnels, using an advanced, object oriented software architecture and parallelized computation techniques. The model takes into consideration all relevant components of the construction process, an automatic model generator (Stascheit et al, 2007) and a three-phase model for partially saturated soils to represent face support by means of compressed air (Nagel, Stascheit and Meschke, 2007).

Figure 3 shows the different components of this simulation model. The shield machine (Fig. 3a(5)), the hydraulic jacks (Fig. 3a(6)) and the segmented lining (Fig. 3a(7)) are considered as separate components. Frictional contact between the shield machine, modelled as a three dimensional deformable

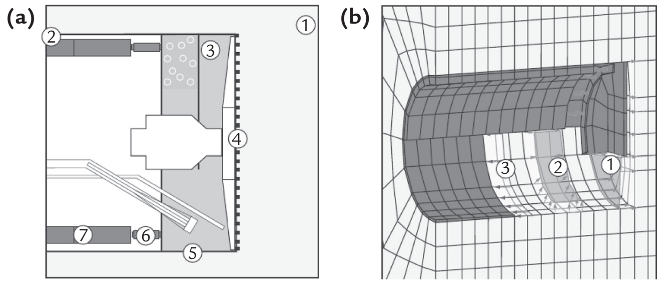

Figure 3 (a) components of the simulation model for shield tunnelling 1: soil, 2: tail void, 3: excavation chamber, 4: cutting wheel, 5: shield skin, 6: hydraulic jacks, 7: segmented lining; (b) loading conditions 1: support pressure, 2: weight of the shield machine, 3: thrust and grouting pressures.

body, and the surrounding soil is accomplished by means of a surface-to-surface contact formulation in a geometrically nonlinear formulation (Laursen, 2002). The heading face support (Fig. 3b(1)) and the tail gap grouting (Fig. 3b(3)) are modelled by means of face loads and prescribed pore water pressures.

The gap between the segmented lining tube and the outer limits of the excavated ground is refilled with grouting suspension, modelled as a fully saturated two-phase material (Fig. 3a(2)). The material model for the grouting mortar is time-variant and accounts for the stiffening behaviour of the mortar. In this formulation the fluid interaction between the grout and the soil and the dissipation of the grouting pressure behind the TBM are taken into account, as well as an initially pressurised fluid state of the grout and its hardening characteristics during hydration.

The hydraulic jacks, modelled as truss elements, are used to steer the shield along the prescribed tunnel alignment. The respective elongation is controlled by an automatic steering algorithm, implemented to keep the TBM on the designed alignment path, similar to the one proposed in (Kasper & Meschke, 2004).

The simulation of the tunnel advance is performed using a step-by-step procedure that consists of two phases: the excavation stage and the lining erection.

A three phase model for partially saturated soil (Fig. 3a(1)) is formulated within the framework of the Theory of Porous Media (TPM) applying the effective stress concept considering large deformations. In terms of this model, the soil consists of phases, the solid soil skeleton (solid phase) and water and air (fluid phases) filling the pore space of the soil. The constitutive relations are described via the soil-water characteristic curve, relative permeabilities and a stress-strain relation for the soil skeleton.

4 NUMERICAL EXAMPLE

In this example the behaviour of pile-soil interaction is considered in a model that consists of a building and its pile foundations and a tunnel that is excavated underneath. The reactions of the building subject to tunnelling induced soil movements are investigated. Without reference to a specific project, the construction of a shallow shield driven tunnel in homogeneous soft cohesive soil, symmetrically underneath the building is simulated. The tunnel is characterized by a diameter D of 4.4 m and a cover depth of 8.17 m. The ground water table is assumed to be at the level of the building foundation plate, 1.8 m below the ground surface. The porosity of the soil is assumed as 20%, and the initial permeability for air flow and water is assumed as $k_0 = 14.4$ cm/h and 144.0 cm/h, respectively. The building is a high-rise residential building, consisting of 12 aboveground storeys and one underground storey, with dimensions of base 16×16 m and a total height of 39.6 m.

This structure is stiffened by an RC core structure located in the centre of the base, and cellar walls acting as a rigid box together with floor and foundation plate. The building is founded on piles, 15 m long, with dimensions of cross-section 0.6×0.6 m, uniformly distributed on the basis of the plate at distances of 4 m each. In this study the pile heads are considered to be totally free of restraint in the form of displacements and rotations. Both building and piles are modelled as linear elastic deformable bodies, with a typical concrete Young's modulus of 30 GPa and a weight of 25 kN/m³.

The analyses were carried out in two steps, where in the first step a model for the in-situ stress state has been calculated such that the equilibrium for element stresses under gravity loading is obtained. In the second phase, the in-situ stresses are transferred to the actual simulation model and the simulation of the shield driven tunnelling process is performed.

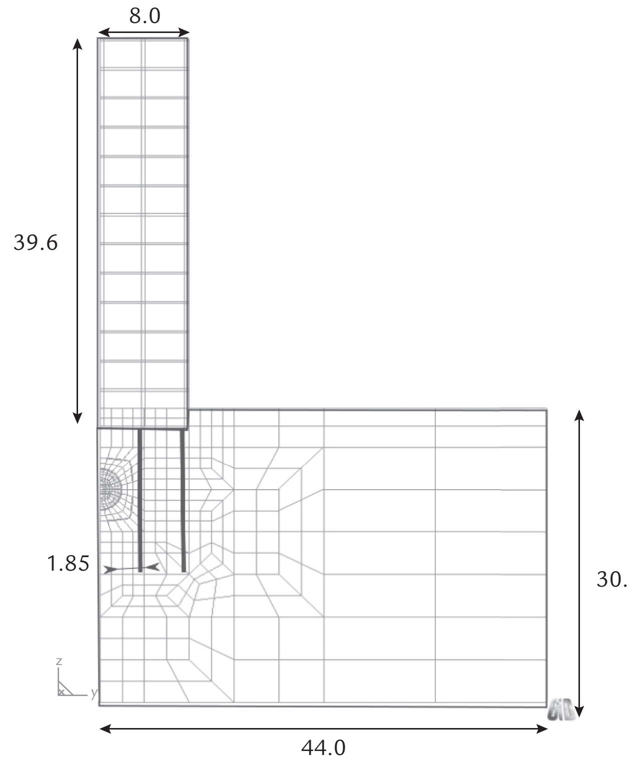

Figure 4 Geometry and FE mesh of the symmetrical model (dimensions in [m]).

4.1 Study of Interactions

In the first case the building is located symmetrically above the prescribed tunnel alignment. The closest pile group in that case is located at only 2 m distance from the tunnel lining. Due to symmetry of the model, only half of domain is modelled, as shown in Figure 4. The tunnelling simulation covers 48 excavation steps, each with a length of 1 m.

In Figure 5, horizontal displacements in two points of the model are compared: one point is located at the tip of the innermost pile while the other point is located at a distance of 1.85 m from the pile. The horizontal displacements are plotted over time while the excavation proceeds.

Negative pile displacements indicate movements towards the tunnel in horizontal direction, and settlements in vertical direction. It can be observed that, in general, the piles undergo the same evolution of deformations as the surrounding ground. However, the soil displacements exhibit a much larger magnitude. This can be explained by the stiffening effect the piles have on the structural behaviour of the soil. Since the bending moments and critical stress states in piles are mostly a consequence of a change of shape, the focus must be put on the pile displacement profile rather than the magnitude of displacements.

In Figure 6 horizontal displacements on top, middle and bottom point of the pile closest to the tunnel are plotted over the excavation steps. It is shown that the tunnel excavation process induces considerable displacements and curvatures in piles when the position of the face of the boring machine is located approx. 2 diameters ahead of the observed pile.

Relative horizontal displacements decrease steadily with depth, thus producing mild changes in curvature of the piles. The maximum induced relative

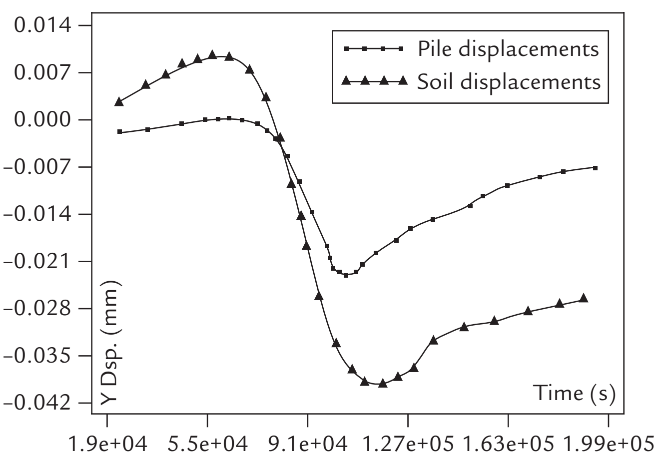

Figure 5 Horizontal displacements of a point at the tip of the innermost pile and a point located at a distance of 1.85 m from the pile plotted over time.

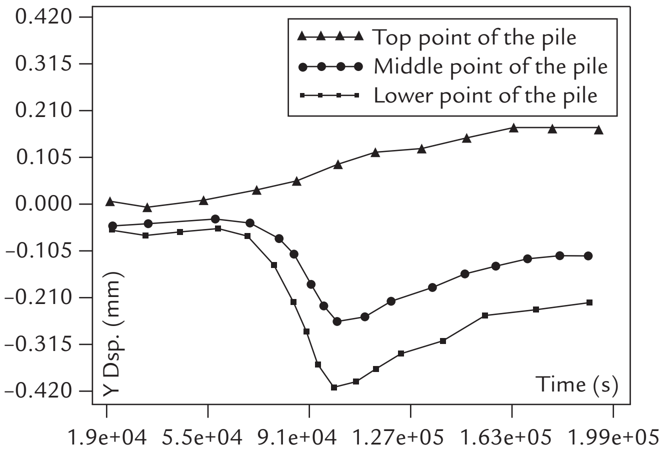

Figure 6 Horizontal displacements of three points located on top, middle and bottom of the pile closes to the tunnel, plotted over the advancing excavation process.

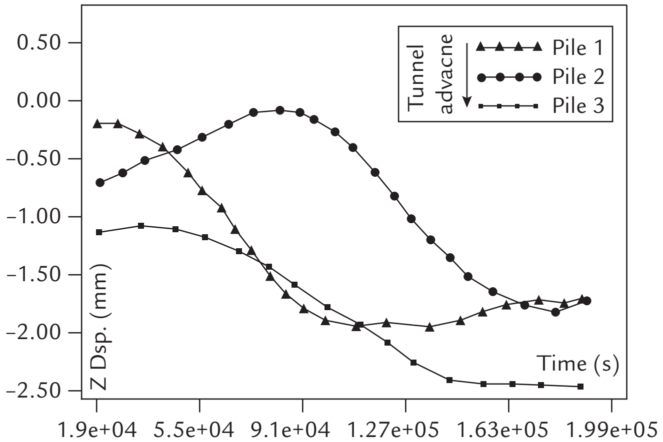

Figure 7 Vertical displacements of the tip of three piles induced by the tunnel construction process.

displacement occurs when the tunnel face passes the pile. The induced curvature reduces slightly after the lining has been installed and the grouting mortar has been injected.

Vertical displacements that occur on the tip of the piles during the shield advancement are shown in Figure 7. Since the displacements are plotted for three piles located along the tunnel axis, it can be seen that the vertical movements of piles follow the inclination of the building backwards in the direction opposite to the TBM advance, due to induced settlements on the soil surface in front of the tunnel face.

This numerical simulation has shown that due to high axial stiffness, the piles settle approximately uniformly along its length.

5 CONCLUSIONS

The soil-pile interaction model developed for the representation of frictional contact between pile and soil elements has been successfully implemented in a process-oriented finite element model for the simulation of the construction process in mechanised tunnelling. This formulation allows to model pile groups independent from the discretisation of the soil.

This complex model takes into consideration all basic components of tunnel-soil-structure interaction: a suitable model for the soil and the building with its foundations, contact between soil and structure and all relevant components involved in shield tunnelling such as the partially or fully saturated soil, the shield machine, the segmented lining, the tail void grouting and the heading face support by means of earth pressure, support liquids or compressed air.

The tunnelling process induces both horizontal and vertical displacements in the surrounding soil and in the pile foundations, thus leading to an inclination of the building atop of the excavated tunnel. Relative displacements along the pile induce a maximal curvature of the piles when the tunnelling machine passes the pile.

It can further be observed that the pile foundations have a stiffening effect on the surrounding soil since they induce bending stiffness to the vicinity of the tunnel.

The proposed model is capable to realistically model the interactions between pile-founded buildings and the mechanised tunnelling process and hence serves as a valuable tool for the prediction of tunnelling-induced settlements of surface structures.

ACKNOWLEDGEMENTS

This work has been partially funded by the DFG Deutsche Forschungsgemeinschaft in the framework of the Collaborate Research Area SFB837 “Interaction modelling in mechanized tunnelling”. Funding to the first author has been granted by the German Academic Exchange Service DAAD—Special Programme for Serbia. This support is gratefully acknowledged.

REFERENCES

Lee, R. G., Turner, A. J. and Whitworth, L. J. (1994). Deformations cased by tunneling beneath a piled structure. Proc. XIII Int. *Conf. Soil Mechanics and Foundation Engineering*. University Press, London, pp. 873–878.

Lee, K. M., Rowe, R. K. and Lo, K. Y. (1992). Subsidence due to tunneling: Part I—Estimating the gap parameter. *Canadian Geotechnical Journal*, Vol. 29, No. 5, pp. 929–940.

Lee, K. M. and Rowe, R. K. (1989). Deformations caused by surface loading and tunneling: the role of elastic anisotropy. *Geotechnique*, Vol. 39, No. 1, pp. 125–140.

Engin, H. K., Septanika, E. G. and Brinkgreve, R. B. J. (2008). Estimation of Pile Group Behavior using Embedded Piles. *12th International Conference of International Association for Computer Methods and Advances in Geomechanics (IACMAG)*, Goa, India.

Coutts, D. R. and Wang, J. (2000). Monitoring of reinforced concrete piles under horizontal and vertical loads due to tunneling. *Tunnels and Underground Structures* (eds. Zhao, Shirlaw & Krishnan), Balkema.

Tham, K. S. and Deutscher, M. S. (2000). Tunnelling under Woodleigh Workers' Quarters on Contract 705. *Tunnels and Underground Structures* (eds. Zhao, Shirlaw and Krishnan), Balkema.

Loganathan, N. and Poulos, H. G. (1998). Analytical prediction for tunneling-induced ground movements in clays. *Journal of Geotechnical and Geoenviromental Engineering*, Vol. 124, No. 9, pp. 846–856.

Chen, L. T., Poulos, H. G. and Loganathan, N. (1999). Pile responses caused by tunneling. *Journal of Geotechnical and Geoenvironmental Engineering*, Vol. 125, No. 3, pp. 207–215.

Loganathan, N., Poulos, H. G. and Xu, K. J. (2001). Ground and pile-group response due to tunneling. *Soils and Foundations*, Vol. 41, No. 1, pp. 57–67.

Mroueh, H. and Shahrour, I. (2002). Three-dimensional finite element analysis of the interaction between tunnelling and pile foundations. *Int. Journal for Numerical and Analytical Methods in Geomechanics*., Vol. 26, pp. 217–230.

Panet, M. and Guenot, A., (1982). Analysis of convergence behind the face of a tunnel. *Proc. Tunnelling 82,* Institution of Mining and Metallurgy, London, pp. 197–204.

Stallebrass, S. E., Grant, R. J. and Taylor, R. N. (1996). A finite element study of ground movements measured in centrifuge model tests of tunnels. Proc. *Int. Symposium on Geotechnical Aspects of Underground Construction in Soft Ground*, London (eds. R. J. Mair and R. N. Taylor), Balkema, pp. 595–600.

Addenbrooke, T. I., Potts, D. M. and Puzrin, A. M. (1997). The influence of pre-failure soil stiffness on the numerical analysis of tunnel construction. *Geotechnique*, Vol. 47, No. 3, pp. 693–712.

Simpson, B., Atkinson, J. H. and Jovicic, V. (1996). The influence of anisotropy on calculations of ground settlements above tunnels. Proc. *Int. Symposium on Geotechnical Aspects of Underground Construction in Soft Ground*, London (eds. R. J. Mair and R. N. Taylor), Balkema, pp. 591–594.

Luenberger, D.G., Linear and Nonlinear Programing. Addison- Wesley, reading, Massachusetts, second Edition 1984.

Stascheit, J.; Nagel, F.; Meschke, G.; Stavropoulou, M. & Exadaktylos, G. (2007). An automatic modeller for finite element simulations of shield tunnelling, CD-ROM *Proceedings of EURO:TUN 2007,* Eberhardsteiner, J.;Beer, G.; Hellmich, C.; Mang, H.A.; Meschke, G. & Schubert, W. (eds.).

Nagel F., Stascheit J., Meschke G. 2007. Three-phase modelling and numerical simulation of shield tunnelling in partially saturated soils, CD-ROM *Proceedings of the ECCOMAS Thematic Conference on Computational Methods in Tunnelling (EURO:TUN2007)* Eds.: J. Eberhardsteiner, G. Beer, C. Hellmich, H.A. Mang, G. Meschke, W. Schubert.

Kasper T., Meschke G. 2004. A 3D finite element simulation model for TBM tunnelling in soft ground. International *Journal for Numerical and Analytical Methods in Geomechanics*, 28, 1441–1460.

T.A. Laursen: Computational Contact and Impact Mechanics, Springer (2002).

Author Query

AQ: Please provide citation for Figure 2.